TALLINNA TEHNIKAÜLIKOOL
TALLINN UNIVERSITY OF TECHNOLOGY

TTÜ Department of Materials and Environmental Technology

# EFFECT OF OZONE ON PHOTOCATALYTIC DEGRADATION OF ACETONE VAPOUR ON P25 $TiO_2$ COATING

## OSOONI MÕJU ATSETOONIAURU FOTOKATALÜÜTILISELE OKSÜDEERIMISELE P25 $TiO_2$ KATETEGA

MASTER THESIS

Student: Irina Petrotšenko

Student code: 177032 KAKM

Supervisor: Marina Kritševskaja, senior lecturer
Co-supervisor: Maarja Kask, early stage researcher

Tallinn, 2019

# AUTHOR'S DECLARATION

Hereby I declare, that I have written this thesis independently.
No academic degree has been applied for based on this material. All works, major viewpoints and data of the other authors used in this thesis have been referenced.

"....." ..... 201.....

Author: Irina Petrotšenko

/ signature /

Thesis is in accordance with terms and requirements

"....." ..... 201.....

Supervisor: Marina Kritševskaja

/signature/

Accepted for defence

"....."..... 201....

Chairman of theses defence commission: .....

/name and signature/

**Department of Materials and Environmental Technology**

# THESIS TASK

**Student**: Irina Petrotšenko, 177032KAKM

Study programme, main speciality: KAKM02/09 - Chemical and environmental technology

Supervisor(s): Marina Kritševskaja, senior lecturer, ph. 620 2851

Co-supervisor: Maarja Kask, early stage researcher, ph. 620 2824

**Thesis topic**:

(in English) Effect of ozone on photocatalytic degradation of acetone vapour on P25 $TiO_2$ coating

(in Estonian) Osooni mõju atsetooniauru fotokatalüütilisele oksüdeerimisele P25 $TiO_2$ katetega

**Thesis main objectives**:

1. Learning about air purification techniques including photocatalytic oxidation theory
2. Conducting experimental series (photocatalysis of acetone vapour in air with P25 $TiO_2$ coating)
3. Analysing the results and writing Master's thesis

**Thesis tasks and time schedule:**

| Nr | Task description | Deadline |
|---|---|---|
| 1. | To study the literature on air pollutants and air treatment methods | 11.2018 |
| 2. | To carry out an experimental part of the Master's thesis - study of photocatalytic activity | 01.2019 |
| 3. | To write a Master's Thesis | 05.2019 |

**Language:** English **Deadline for submission of thesis:** "....."....201….a

**Student:** Irina Petrotšenko ..... "....."....201….a
/signature/

**Supervisor:** Marina Kritševskaja ..... "....."....201….a
/signature/

**CO-supervisor:** Maarja Kask ..... "....."....201….a
/signature/

# Table of contents

# Preface

In this study, the degradation of acetone vapour by photocatalytic oxidation (PCO) with titanium dioxide ($TiO_2$) catalyst under ultraviolet (UVA) and the combination of PCO and ozone ($O_3$) was investigated to evaluate the enhancement effect of $O_3$.

I want to thank my co-supervisor Maarja Kask for the supervising, collaboration in the performance of the experiments in the laboratory, useful comments in the analysis of results.

I would like to express my gratitude to my supervisor Marina Kritševskaja for constructive criticism, points in the direction for progress and useful comments.

Keywords: photocatalytic oxidation, acetone vapour, ozone, P25 $TiO_2$ coating, master's thesis.

## List of abbreviations, terms and symbols

| | |
|---|---|
| A | Activity rate |
| AOP | Advanced oxidation process |
| CAC | Chemically active compound |
| CAGR | Compound annual growth rate |
| E | Calculated emission |
| EF | Emission factor |
| H | Effective stack height |
| PCO | Photocatalytic oxidation |
| PM | Particulate matter |
| Q | Source strength |
| RH | Relative humidity |
| ROG | Reactive organic gases |
| RT | Residence time |
| SRT | Specific residence time |
| SVOC | Semivolatile organic compound |
| u | Average wind speed |
| UV | Ultraviolet |
| VIS | Visible light |
| VOC | Volatile organic compound |
| $\sigma_y$ | Horizontal dispersion coefficient |
| $\sigma_z$ | Vertical dispersion coefficient |

## List of figures

## List of tables

# Introduction

In light of technology development and increase in overall scale production, the need of air purification became one of vexed problems. The pollution of air involves not only air around pollution source, but also the water and soil in the surrounding area. Pollutants have effect on environment both locally and globally, as due to mass transfer they spread.

The air is an integral part of a life, thus the air purification from pollutants is the fundamental problem, where solutions are necessary. There is a number of air treatment methods with certain advantages and disadvantages, but also the developments with input of new technologies and researches are of great interest. The photocatalytic air purification is a one of the most researched and promising methods. It is able to degrade the volatile organic compounds (VOC), while the catalyst films are self-cleaning, thus easy in use and upkeep.

The aim of this study was the degradation of acetone vapour by photocatalytic oxidation (PCO) with titanium dioxide ($TiO_2$) catalyst under ultraviolet (UVA) irradiation in a continuous multi-section reactor. The combination of PCO and ozone ($O_3$) under different operating conditions was investigated to evaluate the enhancement effect of $O_3$.

# 1. LITERATURE REVIEW

## 1.1 Air pollution

### 1.1.1 Air pollutants

It is common knowledge that air quality influences human health. Air pollution is one of the factors that is harmful to our health. Exposure to polluted air may cause various health problems. The symptoms may vary from simple mild irritation of eyes to serious conditions related to diseases. The air we breathe contains a variety of pollutants that are emitted into the atmosphere and could be found outdoors and indoors.

Air pollution can be caused by human activity as well as by natural processes. Polluted air usually contains a mixture of solid particles including windblown dust and pollen, liquid droplets and gases, and mould spores.

The common sources of outdoor air (referred to as ambient air) pollution are from human activity, such as emissions caused by combustion processes from motor vehicles, solid fuel burning, industry, heating appliances, tobacco smoke, while in case of natural sources pollution comes with smoke from bushfires, windblown dust, and pollen and mould spores (biogenic emissions from vegetation). Pollution from natural events depends on the season, weather conditions, number and types of sources.

The most common air pollutants of ambient air include [1]:

- Particulate matter (PM10 and PM2.5)
- Ozone ($O_3$)
- Nitrogen dioxide ($NO_2$)
- Carbon monoxide (CO)
- Sulphur dioxide ($SO_2$)
- Volatile organic compounds (VOCs)

Most of the emissions are from local or regional sources. Due to atmospheric conditions, the air pollution spreads and travels for days, therefore affecting people far away from its original source.

### 1.1.2 Sources of VOC-s

VOCs consist of organic molecules and volatile hydrocarbons (2-10 carbon atoms), which are released into the air. VOCs are chemical compounds that have a high vapour pressure at room temperature. The high pressure is a result of low boiling point that causes large number of molecules to evaporate (or sublimate) from the liquid (or solid) state of the compound and enter the surrounding air. By the European Union definition, the VOC is "any organic compound having an initial boiling point less than or equal to 250 °C measured at a standard atmospheric pressure of 101.3 kPa" [2].

There are different kinds of VOCs that can be found in the air: alkanes, alkenes, alkynes, halogenated hydrocarbons, aromatic hydrocarbons, terpenes, aldehydes, ketones and alcohols. A few of them are toxic or carcinogenic, thus there are restraints for their concentrations in the air. There are two types of sources: biogenic and anthropogenic. It is estimated, that about 5% of the VOCs are emitted from plants (greenery, flora), about 50% from transport, solvent use gives 30% and other industrial processes 15% [3].

The occurring overall VOC flux from natural sources is estimated to be 1150 Tg C. It consists of 44% isoprene, 11% monoterpenes, 22.5% other reactive VOC, and 22.5% other VOC [4]. Considerable doubt prevail for estimated numbers, specifically for compounds other than isoprene and monoterpenes. The rain forests provide about a half of overall natural VOC emissions. Farmlands, fields, forests provide 10-20% individually [4]. Natural VOCs emission sources are also forest fires and volcanic eruptions.

In addition to the above-mentioned transport and industries, cattle farms, coal mining, oil and natural gas extraction are the emissions sources as well. Cow farms could be named as the major source of emissions, as silage and manure are sources of VOCs (Figure 1). Emitted VOCs include alcohols (ethanol is dominant), aldehydes, ketones, esters, ethers, sulfides, carbonyls, aromatics. Some of reactive organic gases (ROG), which are the gases that react in the atmosphere to form the photochemical smog, can cause formation of ground level ozone. The primary ROG source on farm is animal feed, especially silages, other sources are manure storages and land application (e.g. cropland fertilisation) [5].

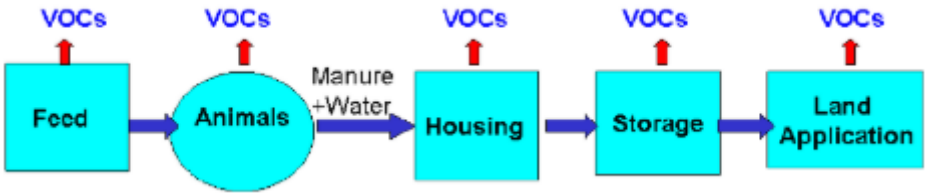


Figure 1. VOCs emission sources on dairy farms [5].

Referring to indoor and outdoor air and generalising: the indoor air can contain VOCs from such common sources as paint, furniture polish, cleaners, laundry detergents, solvents (e.g. nail polish remover with acetone) and thinners (e.g. paint thinner), air fresheners, smoke (from burning stove or candle, cigarettes). From outside of our homes the VOCs sources are: traffic, combustion of gasoline, factories (paints, plastics, petroleum), trash recycling facility (trash burning) and agriculture.

### 1.1.3 Sources of acetone

In present study, acetone was used as model air pollutant. The vapour of acetone is colourless, has a mint-like odour and the smell is perceivable by human senses at approximately 100 ppm [6]. Significant properties of acetone are listed in Table 1. When released into the atmosphere, the acetone will disperse into air (71% by mass) and water (ca. 28% by mass). This percentage was determined by fugacity modelling analysis [7].

Acetone is a VOC and common air pollutant and there are models of diffusion of acetone that let to estimate its diffusion time in ambient air. The acetone production plant located in China can be taken as an example. The plant capacity is about 614000 tons per year and assumed loss of acetone to ambient air is 1% (emission factor) [8-10]. The original calculations in [8] were modified for another value of plant capacity.

Emission rate can be calculated as follows (Equations 1-3):

$$A \times EF = E \tag{1}$$

Where: A – activity rate (for example, the process rate),

EF – emission factor,

E – calculated emission.

For the chosen plant the calculated emission could be calculated as follows:

$$E = \frac{614\,000\ tons}{1\ year} \times 0.01\ = 6140\ [tons\ year^{-1}] \text{ of acetone} \qquad (2)$$

Converting the amount to g $sec^{-1}$ of acetone:

$$\frac{6140\ tons\ of\ acetone}{1\ year} \times \frac{10^6 g}{3.156\ \times\ 10^7\ sec} = 194.55\ [g\ sec^{-1}] \text{ of acetone} \qquad (3)$$

Another assumption is that emissions are not from one-point source, they are from different locations within plant. Therefore, we will assume that the emission source area is 100 square meters and 10 meters high (average emissions height).

Acetone ground level concentrations can be estimated at locations downwind of plant. For that the virtual point source of emissions is assumed to be upwind. As the acetone molecules occur in air, that has certain direction of flow, they start the process of distribution in flowing air mass (dispersion process). This process is described by Gaussian dispersion model [11]. This model describes concentration distribution in crosswind and in vertical direction, centred at the line downwind from the source (Figure 2). As the distance increases the dispersion also increases.

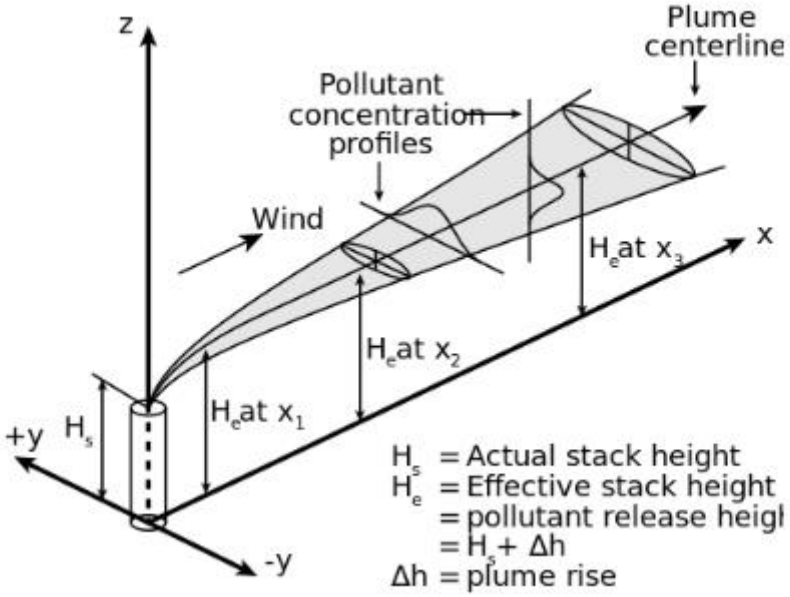


Figure 2. Schematic figure of a Gaussian plume [11].

The distance of crosswind mixing of pollutant is described with horizontal dispersion coefficient, $\sigma_y$. The distance of vertical mixing of the pollutant is described with $\sigma_z$. These coefficients depend

on value of downwind position x and atmospheric stability conditions. The values of $\sigma_y$ and $\sigma_z$ can be found by using Pasquill-Gifford (P-G) Curves (Figures 3 and 4).

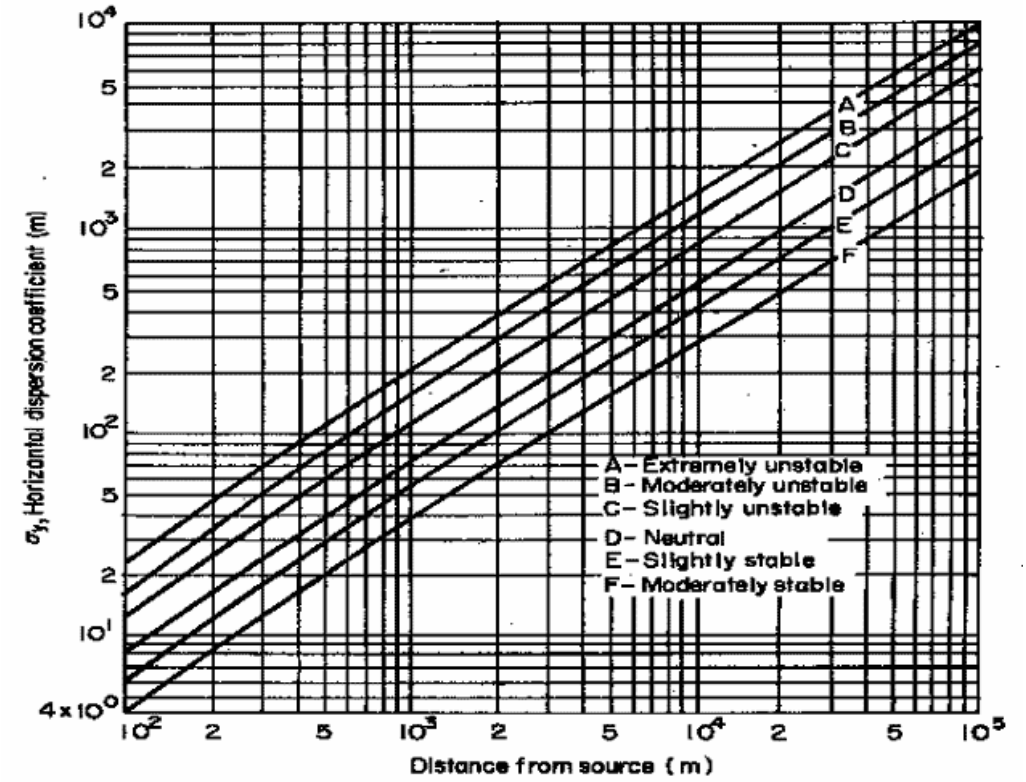


Figure 3. Numerical values of horizontal dispersion coefficient ($\sigma_y$) [12].

Another assumption involves weather conditions. Presume slightly unstable conditions, light wind 2 m $sec^{-1}$ and 10 min of wind not changing its direction, meaning the distance is 1200 m. By Pasquill-Gifford Curves the value of $\sigma_y$ is about 120 m and the value of $\sigma_z$ is about 70 m. Also, the nearest receptor might be 500 meters from the virtual point of source for example. Then ground level concentration might be calculated (Equations 4-7) [8]:

$$X = \frac{Q}{u \times \pi \times \sigma_y \times \sigma_z} \times e^{-\frac{1}{2}\left(\frac{H}{\sigma_z}\right)^2} \quad (4)$$

Where: Q – source strength (same as calculated emission)

u – average wind speed

$\sigma_y$ – horizontal dispersion coefficient

$\sigma_z$ – vertical dispersion coefficient

H – effective stack height

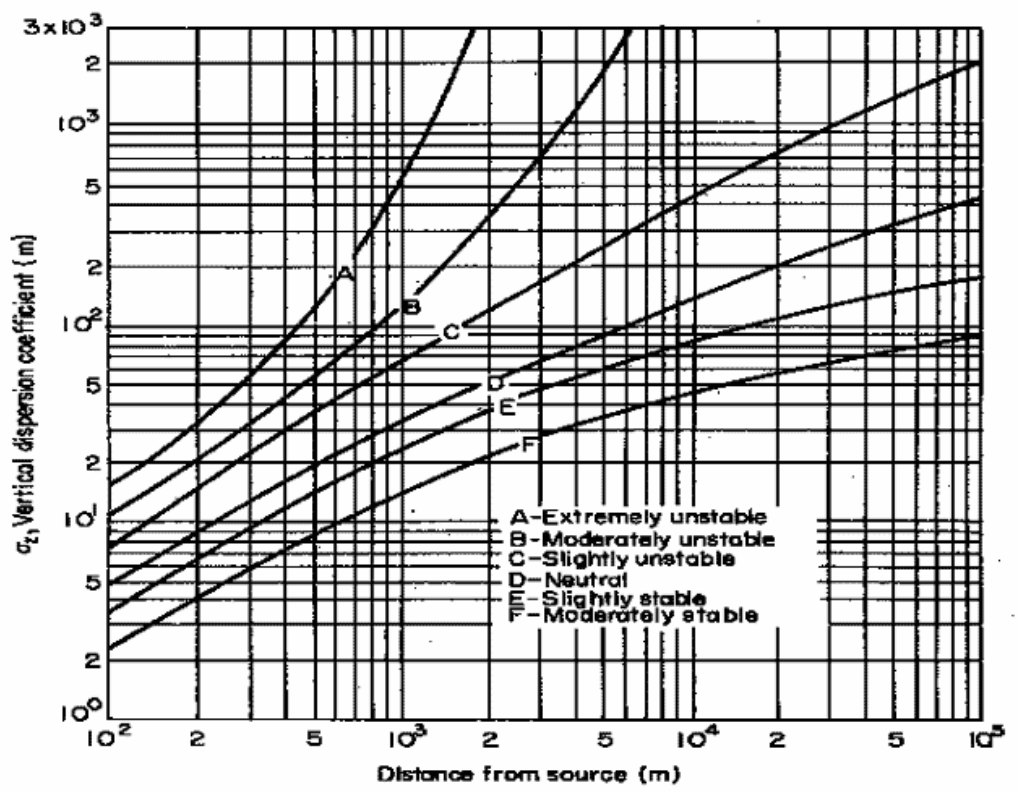

Figure 4. Numerical values of vertical dispersion coefficient (σz) [12].

$$X = \frac{194.55}{2 \times \pi \times 120 \times 70} e^{-\frac{1}{2}\left(\frac{10}{70}\right)^2} = 0.00365\ [g\ m^{-3}] = 3.65\ [mg\ m^{-3}] \quad (5)$$

The result is for a 10-minute emission. For an hour period the value will be:

$$\frac{3.65\ \times 60}{10} = 21.9\ [mg\ m^{-3}] \quad (6)$$

Converting the result to ppm using essential properties of acetone (Table 1):

$$\frac{21.9\ mg\ m^{-3} \times 0.422\ ppm}{1\ mg\ m^{-3}} = 9.24\ [ppm] \quad (7)$$

Thus, relatively high concentrations of acetone could be monitored around the acetone production plants.

Table 1. Some essential properties of acetone [8].

| | |
|---|---|
| Synonyms | dimethyl ketone, 2-propanone |
| Chemical formula | 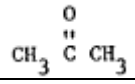 |
| Molecular weight | 58.08 g $mol^{-1}$ |
| Boiling point | 56.5 °C |
| Melting point | -95.6 °C |
| Specific gravity | 0.792 at 20° / 4 °C |
| Vapour density | 2.00 (air = 1) |
| Solubility | Soluble in all proportions in water, alcohol and ether |
| Explosive limits | 2.5 to 12.8 percent by volume |
| Ignition temperature | 560 °C |
| Flash point | -17.8 °C (closed cup) |
| At 25 °C and 760 mm Hg | 1 ppm vapour = 2.372 mg $m^{-3}$<br><br>1 mg $m^{-3}$ vapour = 0.422 ppm |

In a report on analysis of the global acetone market a forecast was made for market development for the near future. The report covers all global regions and 133 countries. The estimated production of acetone is 7,666 thousand tons by the end of 2023, with compound annual growth rate (CAGR) about 2% per year during 2017-2023 period [13]. At the same time the rate of acetone use for production of bisphenol A considered to be 20% of total acetone production volume [13]. Use of acetone for isopropanol production grows at 18.22% per year [13]. In comparison – the production of acetone in 1974 at 12 plants was approximately 2 billion pounds (~ 907185 tonnes) [8].

The primary sources of emissions are manufacturing industries that make protective coatings, using acetone as a solvent that evaporates into the atmosphere. Other sources and estimated emissions are: production of pharmaceuticals, chemical processing solvents, cellulose acetate

spinning solvents, acetone manufacturing (considered 1% loss), absorbent packing for acetylene, bulk storage, manufacturing of methyl methacrylate and bisphenol A (BPA) (considered 1% loss) [8].

### 1.1.4 Sources of ozone

Ozone ($O_3$) is a gas, composed from three oxygen atoms. Significant properties of gaseous ozone are listed in Table 2. It appears in the upper atmosphere and at ground level of Earth. Depending on its whereabouts, the ozone can be considered “good” or “bad”.

Table 2. Significant properties of gaseous ozone [14]

| | |
|---|---|
| Synonyms | trioxygen |
| Molecular weight | 47.997 g $mol^{-1}$ |
| Density | 2.141 kg $m^{-3}$ (at 1.013 bar and 0 °C) |
| Critical temperature | 112.2 °C |
| Critical pressure | 55.73 bar |
| Critical density | 540 kg $m^{-3}$ |
| Colour | Pale blue |

The “good” $O_3$ is called stratospheric ozone (15 - 50 km) and forms the largest fraction. It is located in the upper atmosphere and occurs naturally [15]. This formed layer shields the surface of the earth from UV-rays.

The tropospheric $O_3$ on ground-level (0-15 km) is a secondary hazardous air pollutant, as it is not emitted directly, but is formed in chemical reaction between oxides of nitrogen (NOx) and VOCs. This $O_3$ is treated as harmful due to it being a main component of smog and its negative effects on humans and the environment [15].

Under typical conditions of daytime and well mixed air mass in the atmosphere, four chemical reactions in the stratosphere occur rapidly, constantly and maintain an ozone layer and are called Chapman cycle (Equations 8-11) [16]:

$$O_2 + hv \rightarrow O + O \quad (8)$$

$$O + O_2 \rightarrow O_3 \quad (9)$$

$$O_3 + hv \rightarrow O_2 + O \quad (10)$$

$$O + O_3 \rightarrow O_2 + O_2 \quad (11)$$

And in troposphere occur another three chemical reactions (Equations 12-14):

$$NO_2 + hv \rightarrow NO + O \quad (12)$$

$$O + O_2 \rightarrow O_3 \quad (13)$$

$$NO + O_3 \rightarrow NO_2 + O_2 \quad (14)$$

These processes do not result in net gain of the ozone. There are two chemical components of the troposphere that lead to ozone formation: VOC and NOx. Formation of ozone is initiated by reaction of VOCs or CO with $^{\bullet}$OH radical. Reaction is followed by NO conversion to $NO_2$ as a result of a reaction with $HO_2^{\bullet}$ or $RO_2^{\bullet}$ radicals, generating $^{\bullet}$OH (Equations 15-18) [17]:

$$VOC + {}^{\bullet}\mathrm{OH} \xrightarrow{O_2} RO_2^{\bullet} + H_2O \quad (15)$$

$$CO + {}^{\bullet}OH \xrightarrow{O_2} HO_2^{\bullet} + CO_2 \quad (16)$$

$$RO_2^{\bullet} + NO \xrightarrow{O_2} Secondary\,VOC + HO_2^{\bullet} + NO_2 \quad (17)$$

$$HO_2^{\bullet} + NO \rightarrow {}^{\bullet}OH + NO_2 \quad (18)$$

The reactions 17 and 18 lead to the formation of ozone through the reactions 12 and 13.

The chemical reactions of $O_3$ formation are not instant, they take hours or days. Considering the mass movement in air, the maximum concentrations can occur downwind of the VOC and NOx emissions source area (Figure 5).

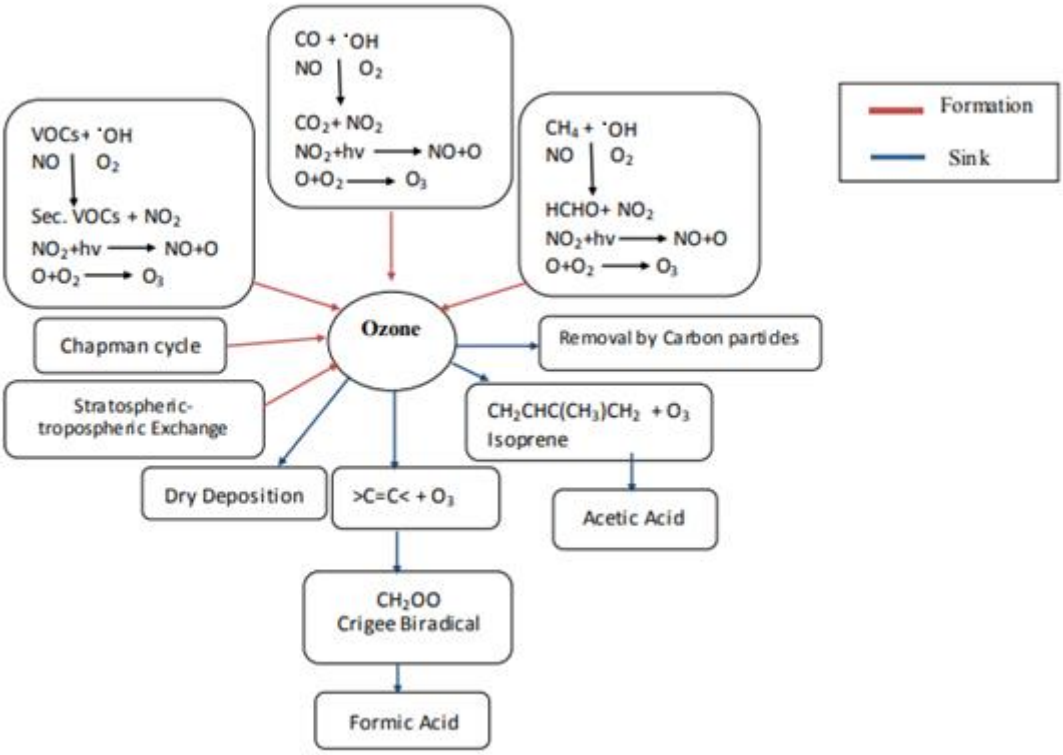


Figure 5. Schematic diagram of different processes of formation and loss of ozone in the troposphere [17].

Aside from industrial sources of the VOC and NOx, the natural sources also take part in $O_3$ generation. The summary of natural and anthropogenic sources of VOC and NOx is presented in Table 3.

Table 3. Summary of natural and anthropogenic sources of VOC and NOx

| **NOx** | | **VOC** | |
|---|---|---|---|
| **Natural** | **Anthropogenic** | **Natural** | **Anthropogenic** |
| Soil, natural fire | Transport (road, sea and rail), power stations, other industry and combustion processes | Vegetation, natural fires | Transport, combustion processes, solvents, oil production |

### 1.1.5 Abatement methods of VOCs

There are several abatement methods of VOCs from air [18], such as:

- Physical methods (condensation, absorption, adsorption)
- Combustion based methods (non-catalytic process, catalytic process)

Physical methods can be used as a single process or in a series.

In the condensation method, influent gas that contains VOCs is directly or indirectly cooled to a point of dew. As a result, some VOCs are condensed, depending on the coolant temperature in the inlet. Use of condenser allows to recover valuable organics or reduce the concentration of VOCs in gas. This unit may be used, when the concentration is relatively high (>1%) in a waste gas stream [19]. Depending on VOCs concentration in the inlet and coolant temperature, the efficiency of removal can be 50-90% [18]. If the VOC concentration levels in the emissions are low (ppm or sub ppm), then absorption method is preferred [19].

In the absorption method, the scrubber with high-boiling organic liquid (usually oil) is used. The scrubber can be a packed tower, a sieve plate tower or a spray chamber. Usually, the counter-current scrubbing process is used, although a recurrent process can also be used. During the absorption process, the VOCs are dissolved in a solvent. Depending on the initial concentration of VOCs, the solvent temperature and the gas to solvent mass ratio, the solubility in the solvent of 90% and more can be achieved [18].

In the adsorption method, sorbent particles are used. The influent stream containing VOCs passes through a bed of adsorbent (granulated activated carbon for instance). The molecules of VOCs are retained on adsorbent surface, micro and macro-pores. The rate of a process declines as the number of active sites of sorbent particles decreases. After reaching a breakpoint, the process is stopped and the bed is regenerated. Desorption is held by passing steam or hot gas through the bed. Desorbed VOCs are recovered by the condensation process. In case if VOC molecules are strongly attached to the surface of particles, the regeneration is made by high-temperature air-oxidation. As a result, the molecules are converted to $CO_2$ and $H_2O$. The efficiency of the process is about 95%, depending on operating temperature and pressure, adsorption-regeneration cycle duration, the concentration of VOC and its type [18].

Combustion-based process has high efficiency of VOC removal (about 98%) [18]. Products of this process are $CO_2$, $H_2O$, $NO_x$ and $SO_2$. Last two products may not be produced.

The non-catalytic process is held at high temperature (800-1100 °C) [18]. The process can be carried out in five ways: direct incineration, recuperative oxidation, regenerative oxidation, flares, oxidation in existing boilers and process heaters.

The process of direct incineration is performed in a combustor with a supplementary fuel-fed burner. The fuel demand depends on the calorific value of VOCs in the burned gas [18].

In the system of recuperative oxidation, the influent gas with VOC is pre-heated before entering into a combustor by exchanging heat indirectly with the withdrawn flue-gas. As a result of heat exchange, the demand of supplementary fuel would be lower. Heat recuperation has a thermal yield of 50 – 80%. Welding joints on hot side of exchanger must be periodically repaired, causing high maintenance costs. Thus, some companies switch to a thermal regenerative system - it has lower maintenance and fuel costs [20].

The regenerative oxidation system has a combustion chamber and two packed hot beds. Those beds contain beads of ceramic or other materials. The influent stream, containing VOCs (concentrations about or slightly below of 1000 ppm), passes through hot bed and gets heated while the bed temperature decreases. After heating the gas is directed into combustor. After combustion reaction the flue gas will be directed to the second bed. Passing through the second bed, the gas temperature will decrease while heating the bed. The beds are used cyclically, in other words the gas flow process is reversed at known intervals of time. This system has a high heat recovery, about 98%, meaning that no additional fuel would be needed or a relatively small quantity [21].

In flaring process the VOC containing gas is burned in an open flame in open air. This method is suitable for gas with high flow rate and calorific value more than 2600 kcal $Nm^{-3}$. The VOC abatement is > 98%. However, heat cannot be recovered and undesired by-products can be produced (noise, smoke, heat radiation, light, sulphur oxides (SOx), nitrogen oxides (NOx), carbon monoxide (CO)) [18, 22].

For VOC incineration the existing boilers or process heaters can also be used. The benefit of the system is that there is no capital expenditure and supplementary fuel is not needed. The disadvantage – the system cannot function with large alterations in gas flow rate and its calorific value (performance is affected if gas calorific value is less than 1300 kcal $Nm^{-3}$ [18].

The catalytic process is carried out at a lower temperature (400-500 °C), therefore the influent gas is preheated to 26-480 °C prior to being directed to combust chamber. Usually, for catalyst the oxides of platinum, copper or chromium are used [18].

Thus, physical treatment methods that do not lead to the degradation of gas-phase pollutants require secondary treatment of formed wastes or purification and reuse of separated organic compounds. Thermal processes are usually economically unfavourable, if gas streams contain low amounts of organic compounds (e.g. less than 100 ppm).

## 1.2 Photocatalytic oxidation

### 1.2.1 Air treatment by photocatalytic oxidation

The photocatalytic oxidation (PCO) is a technology that can be applied for air purification. It is capable to destroy organic particles with sizes of about 0.001 microns, microbes, VOCs, and chemically active compounds (CACs) [23]. The photocatalytic degradation process with titanium dioxide ($TiO_2$) as a catalyst is widely studied for the treatment of wastewater contaminated with organics. In this process a complete mineralization of organic contaminants is achieved under ambient pressure and ambient temperature [24].

The "photocatalysis" term consists from two Greek words: "photo" and "catalysis" (light and acceleration). From those two words the principle of the process is explained – the PCO process consists from a series of radical reactions that occur, when photocatalyst is irradiated by the light with certain energy, usually so-called soft UV or UVA radiation (Figure 6). The most extensively studied photocatalyst is $TiO_2$ (titanium(IV) oxide or titania) on account of its stability, non-toxicity, high photo-activity, suitable band gap structure and low cost [23].

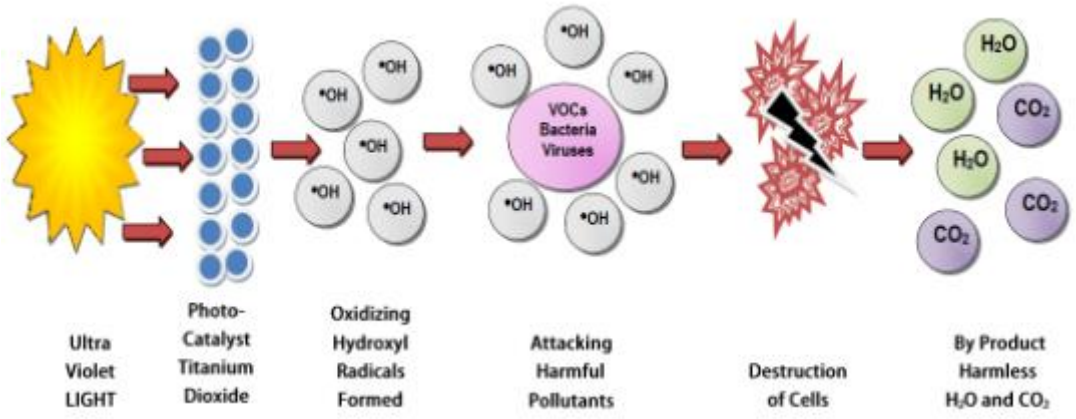


Figure 6. Photocatalytic oxidation process [23].

In nature, minerals of $TiO_2$ occur in three crystal forms: anatase, rutile and brookite (Figure 7). All three forms are built from distorted $TiO_6$ polyhedral units, the difference between them is in units connection ways [25]. The anatase and brookite forms are metastable phases - under high pressure or heat (over 500-600 °C) they would transform into the thermodynamically stable rutile phase. The $TiO_2$ synthesis often result in anatase form with the size of crystals ranging from 6 to 30 nm [25]. The rutile form is stable, when crystals are obtained at a larger size (over

30 nm) and synthesis usually results in rod-like products with the primary crystal size above 35 nm, which is adverse to photocatalytic activity [25]. The brookite form is rarely found in pure phase, thus, there are certain difficulties in studying of this form. As a result, the anatase form is the most researched form of titanium dioxide and it was found to be the best for photocatalytic applications.

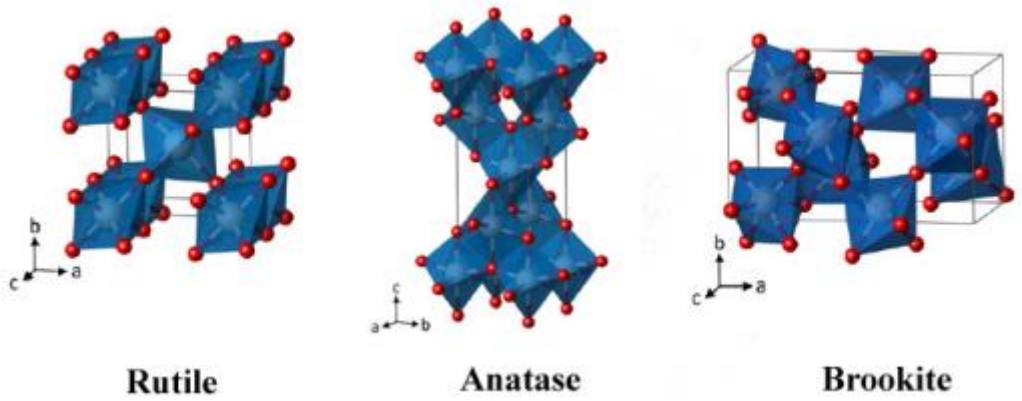


Figure 7. TiO2 crystal structure forms: rutile, brookite and anatase [26].

The 390 nm wavelength of a UVA light has enough energy (UV makes up 5% of the solar energy) to excite atoms in the catalyst, as the $TiO_2$ can be activated by UVA alone (the bandgap is 3.2 eV, Table 4) [23]. The exited form of semiconductive material causes a release of electrons from the valence band to the conduction band, which means that the electrons in it are in two states: free and bound. The "free" electrons move along the crystal frame, formed by $Ti^{4+}$ cations and $O^{2-}$ oxygen anions. The "bound" electrons are bound to the ions of the crystal frame and participate in chemical bond formation. As the $TiO_2$ catalyst absorbs the UV energy, the electrons cross from a bound state to a free state: the free electrons and electron vacancies are formed. The vacancies have a high reactivity that enables to decompose the VOCs [27]. Generally, the PCO process is used for VOCs removal from the polluted air. During this reaction the VOCs are oxidized to $H_2O$, $CO_2$ or any inorganic nontoxic substance by hydroxyl ($^{\bullet}OH$) or superoxide anion ($^{\bullet}O_2^-$) radicals [29].

Table 4. Some bandgap energies of common semiconductors [24].

| Semiconductors | Bandgap energy (eV) | Semiconductors | Bandgap energy (eV) |
|---|---|---|---|
| Diamond | 5.4 | $WO_3$ | 2.76 |
| CdS | 2.42 | Si | 1.17 |
| ZnS | 3.6 | Ge | 0.744 |
| ZnO | 3.436 | $Fe_2O_3$ | 2.3 |
| $TiO_2$ | 3.2 | PbS | 0.286 |
| CdS | 2.582 | PbSe | 0.165 |
| $SnO_2$ | 3.54 | $ZrO_2$ | 3.87 |
| CdSe | 1.7 | $Cu_2O$ | 2.172 |

The basic principle of PCO could be presented by the reactions as follows: the UV light reaches the $TiO_2$ surface, excites atoms in the catalyst and as a result the electrons are released (Equation 19) [28].

$$TiO_2 + hv \rightarrow TiO_2(e_{CB}^- + h_{VB}^+) \quad (19)$$

The released electrons interact with water molecules (water vapour is in the air), and decompose them forming hydroxyl radicals ($^{\bullet}OH$). These radicals are uncharged forms of hydroxide ions ($OH^-$) (Equation 20) [27].

$$TiO_2(h_{VB}^+) + H_2O \rightarrow TiO_2 + H^+ + {}^{\bullet}OH \quad (20)$$

Then, the hydroxyl radicals react with VOC molecules, destroying their chemical bonds. As a result, the carbon dioxide and water are formed. During the reaction, by-products may be formed, as the oxidation could be only partial or the intermediates react with themselves. The by-products may be more dangerous than original components of the reaction (Equation 21) [28].

$$VOC + O_2 + {}^{\bullet}OH \rightarrow H_2O + CO_2 + \text{other products} \quad (21)$$

As any technology, the PCO has its own advantages and disadvantages. The undoubted advantages of the photocatalytic process are the ability to operate at low temperature and pressure, low cost and low energy consumption. If PCO system applies stationary catalytic coatings, the post-treatment stages are not needed. However, due to immobilisation, the process is limited by mass transfer and is characterized by the loss of photocatalytic activity, as the amount of fixed catalyst is usually smaller than, when used in suspension [24]. Another disadvantage of PCO is that oxidation rates and the process efficiency are highly dependent on the operation conditions of photodegradation process. For example: amount and structure of photocatalyst, temperature of reaction medium, time of irradiation, the intensity of light, surface area of photocatalyst. With the increase in photocatalyst surface area the number of active sites is increased, thus the overall process rate also increases. The maximum efficient photodegradation of organic compounds was observed at low concentrations of organics; the decomposition efficiency also depends on the affinity (e.g., adsorption) of organic compounds towards the catalytic coatings. For the maximum process rate, the temperature of reaction should not be greater than 80 °C. The UVA light (up to ca. 400 nm) should have enough energy to excite electrons to exit from valence band to conduction band; the light energy should be greater or equal to the band gap energy [29].

The study of PCO of gas-phase acetone (50–750 ppmv) in air on $TiO_2$-coated optical fibres was made [30]. The conversion of 80% was achieved at conditions of ambient temperature and pressure. The optical fibres were used as a light transmitter and support for catalyst. In the process of acetone conversion to $CO_2$, the intermediates were not detected and the reaction showed a zero-order kinetic behaviour. During the study, it was detected that the light was exponentially extinguished along the coated fibre. Most of the light was absorbed in the front part of the fibre, less than 5 cm [30]. Also, it was noted that the PCO reaction was directly proportional to light intensity. Further, the study showed that optimal coating thickness for optical fibres was between 1 and 2 μm and increase in number of coatings reduced the conversion [30].

### 1.2.2 Combination of photocatalytic oxidation and ozone

With some organic substances, like toluene and others aromatic compounds, the performance of photocatalytic process is not enough for total degradation of pollutant [31]. For reaction enhancement, the ozone can be added to the process. The choice of additional reagent is based

on creating additional pathways for compound degradation, such as UVA/$O_3$ and $O_3$/UVA/$TiO_2$ besides UVA/$TiO_2$.

Several experimental studies were carried out to investigate the influence of ozone ($O_3$) addition to the PCO process for the removal of different compounds [29, 32]. The titanium dioxide is usually used as a catalyst for PCO under UV or VIS. The evaluation of process enhancement was made by the addition of ozone to the process after receiving the results of the initial unmodified PCO study. Also, the experiments were carried out at different relative humidity (RH) values.

Study of d-limonene degradation at different concentrations and RH (0.5–9 ppm and 20 – 80%, respectively) showed an increase in process efficiency up to 12% with the addition of 120 ppb of ozone to the process. d-Limonene is an indoor gaseous biogenic VOC that can react with $O_3$. The reaction generates secondary organic pollutants and aerosols. Addition of $O_3$ to the photocatalytic system reduced the amount of reaction intermediates along with the increase in VOC removal efficiency [32].

Another study of PCO combination with ozone for the removal of formaldehyde and toluene was carried out in dry air (RH 0 to 2%) and higher ozone concentrations (from 20 to 370 ppm of $O_3$) [32]. The results showed the increase in the removal of formaldehyde (from 64 to 97.5%) and toluene (from 12 to 96%), improved durability of the catalyst, as well as the process stability under variation of humidity and $O_3$ concentrations [33].

The study of toluene removal from the air by various combination of methods, i.e., PCO ($TiO_2$/UV), the combination of ozone and PCO ($TiO_2$/UV/$O_3$), and the UV/$O_3$ system was performed [31]. The concentration of $O_3$ varied from 3.3 to 15 ppm, concentration of toluene varied from 1 to 9 ppm, RH varied from 5 to 80% and gas flow rates from 200 to 1200 mL $min^{-1}$. The rates of oxidation of toluene in the $TiO_2$/UV/$O_3$ and UV/$O_3$ experimental series were proportional to the concentrations of ozone and increased with the raise of toluene concentration. However, oxidation rate of toluene and $CO_2$ yield depended also on the combination of processes as follows: $TiO_2$/UV/$O_3$ > $TiO_2$/UV > UV/$O_3$. Besides, it was shown that ozone was removed along with pollutant in $TiO_2$/UV/$O_3$ and UV/$O_3$ reactions [31].

# 2. MATERIALS AND METHODS

## 2.1 Experimental setup

The experimental setup for research consists of two flow meters, a humidifier, a cylinder for preparing an air-organic mixture, a pump, an infrared spectrometer INTERSPEC 200-X FTIR and a multi-section reactor (Figures 8, 9). The PCO reaction took place in sections of a reactor that consists of five 130-ml reactors arranged in series (Figure 8). A thermocouple was mounted in to the first section of reactor for the monitoring of temperature.

In each section of a reactor, a thin film of P25 $TiO_2$ photocatalytic coating on a glass plate was placed. The surface area of the catalytic coating in one reactor section was 120 $cm^2$ and for five sections of a reactor, the total photocatalytic surface area was 600 $cm^2$.

As the light source – a 15 W Philips Actinic T8 lamp (3.5 mW $cm^{-2}$) was located above each section.

For ozone generation process in the setup a GPH287T5VH/4 lamp with the UV-C output at 254 and 185 nm was used. Ozone concentration in air was measured to be about 100 µg $l^{-1}$ at overall air flow rate of 1 l $min^{-1}$ and 150 µg $l^{-1}$ at overall air flow rate of 0.5 l $min^{-1}$.

The temperature in the reactor sections was 44±1 °C measured by thermocontroller (Omega CN9000A) equipped with a thermocouple; the temperature was constant maintained by the heat of lamps covered by light reflectors.

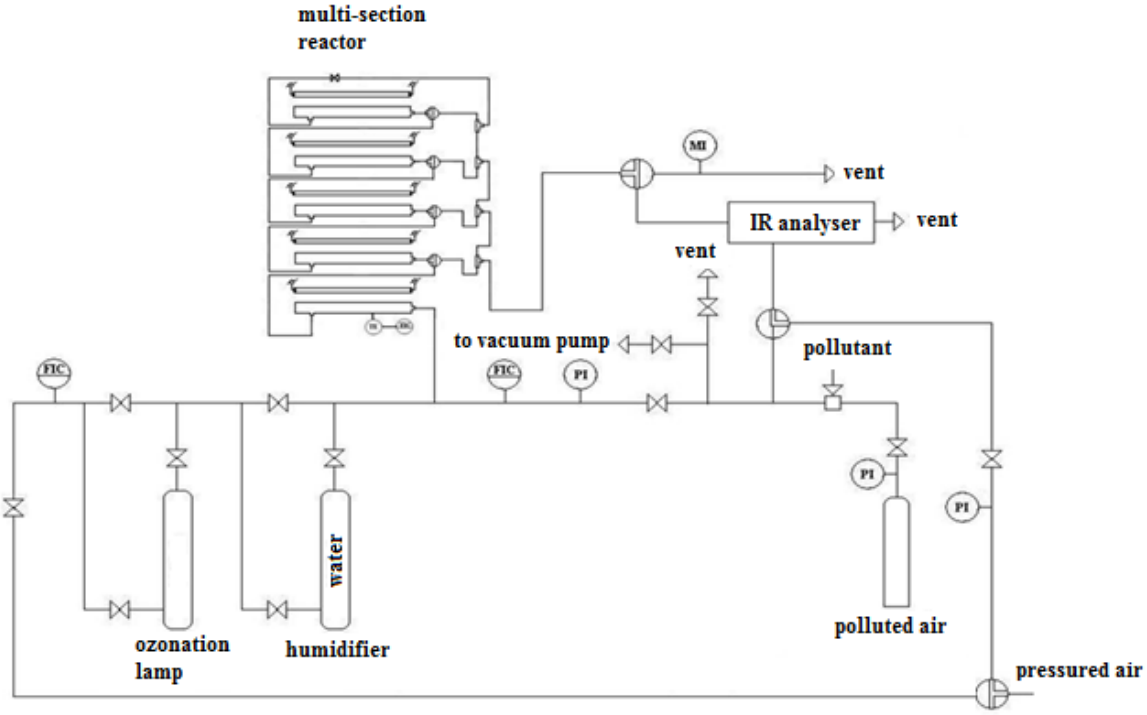


Figure 8. Experimental setup scheme (FIC - flow meter, PI - pressure gauge, MI - moisture meter).

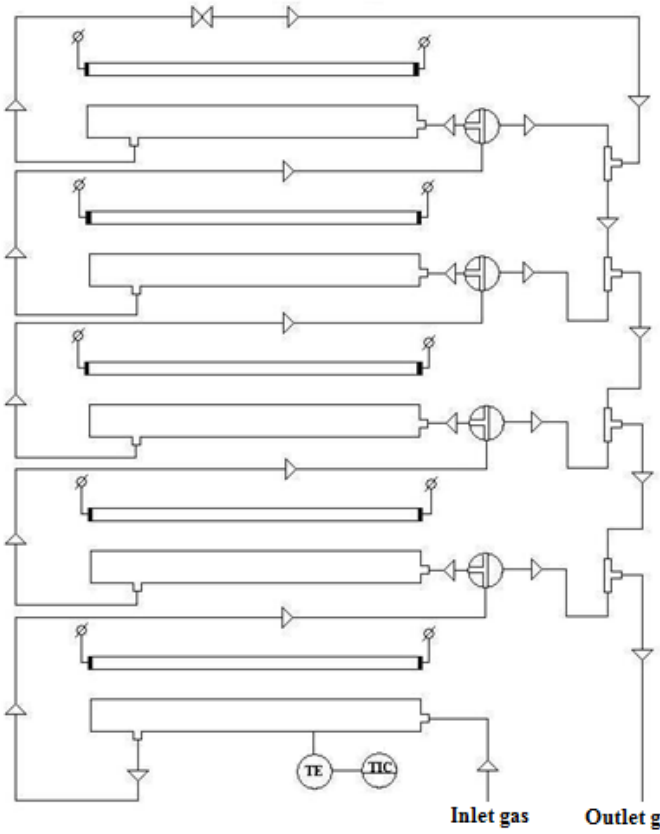


Figure 9. Scheme of a multi-section gas-phase photocatalytic reactor (TE - thermocouple, TIC - temperature controller).

## 2.2 Preparation of photocatalytic coating

The P25 $TiO_2$ photocatalytic coatings were used during the experimental study. The coatings were synthesized by Maarja Kask, early stage researcher at Tallinn University of Technology.

Titanium dioxide P25 is produced by Evonik. P25 contains more than 70% of anatase [34]. For the preparation of coatings, the 5 wt.% slurry was made with ethanol and then sprayed on a glass plate using air brush (Stanley, 150119XSTN) mounted to the compressed air line. Each glass plate has surface of 120±2 $cm^2$. These were coated 15 times to get the specific mass of catalyst of 1.4±0.2 mg $cm^{-2}$. After each spraying the plates were left to air-dry.

## 2.3 Experimental procedure

Acetone-air gas mixture was prepared in 50 litre cylinder. The acetone (Merck, ≥99%) amount (in microliters) required for the desired concentration of gaseous pollutant in air was calculated using the Injection calculator (Equation 22):

$$V[\mu l] = \frac{\left(\frac{P+14.7}{14.7}\right) \times V_{tank}}{R \times (T+273.15)} \times \mathrm{M} \times \mathrm{C}_m \times \frac{0.000001}{\rho \times 0.001} \quad (22)$$

Where: P – filling pressure, 44 psig

$V_{tank}$ – cylinder volume, containing polluted air, 50 litres

R – gas constant, 0.08206 l atm $mol^{-1}$ $K^{-1}$

T – temperature, °C

M – acetone molecular weight, g $mol^{-1}$

$C_m$ – target concentration, ppm

ρ – acetone density, g $ml^{-1}$

In cylinder, vacuum was made by means of vacuum pump. Then, calculated amount of acetone was injected through membrane in to the cylinder. After 20 minutes from the moment of injection, the cylinder was filled with air up to pressure of 3 bars (44 psig). Then, the cylinder was left for 1.5 hours for mixture stabilisation.

The experiments of the PCO of acetone were carried out at different conditions: varied acetone concentrations (20, 40 and 60 ppm), presence and absence of ozone, varied relative air humidity (RH 5 and 40%), specific residence time (0.065 and 0.13 s $cm^{-2}$) and flow rate (1 and 0.5 l $min^{-1}$). The details of the calculation of specific residence time are presented below in the Results and Discussion section. Before each set of experiments, a spectrum of clean air was obtained as a reference (zero) line by using the FTIR spectrometer. The control of the inlet concentration of

the pollutant in air flow was determined through the by-pass line. After 10 and 20 minutes from the beginning of the experiment, the infrared (IR) spectrum of polluted air was gained and analysed. Depending on the result, the next section of reactor with catalytic coating was added to the system enlarging the catalytic surface area and prolonging the overall residence time.

The acetone peaks were measured in the IR range of 1250 - 1177 $cm^{-1}$. The intermediate gaseous products of PCO of acetone were also monitored by FTIR spectrometer. The spectra were taken using Interspec 3.40 Pro software and then processed with Essential FTIR software.

# 3. RESULTS AND DISCUSSION

In present study, the polluted gas flowed through 130-ml sections of reactor with gas flow rates of either 0.5 l $min^{-1}$ or 1 l $min^{-1}$. Thus, according to the Equations 23, 23a, 23b, the time that each molecule of gas was in the reactor section, i.e. residence time or RT, was as follows:

$$Residence\ time = \frac{Section\ volume}{Flow\ rate} \tag{23}$$

$$RT_1 = \frac{130\ ml}{0.5\ l\ min^{-1}} = \frac{130\ ml}{500\ ml\ min^{-1}} = 0.26\ min \quad = 15.6\ [s] \tag{23a}$$

$$RT_2 = \frac{130\ ml}{1\ l\ min^{-1}} = \frac{130\ ml}{1000\ ml\ min^{-1}} = 0.13\ min \quad = 7.8\ [s] \tag{23b}$$

Specific residence time (SRT, equations 24) is calculated using particular surface area of the catalyst in the section of reactor. In this work, the catalyst surface is 120 $cm^2$.

$$Specific\ resident\ time = \frac{Residence\ time}{Catalyst\ surface\ area} \tag{24}$$

$$SRT_1 = \frac{15.6}{120} \ = 0.13\ [s\ cm^{-2}] \tag{24a}$$

$$SRT_2 = \frac{7.8}{120} = 0.065\ [s\ cm^{-2}] \tag{24b}$$

For the assessment of influence of SRT, air humidity and inlet concentration of acetone the pollutant's conversions were calculated (Equation 25):

$$Conversion(\%) = \frac{C_{in} - C_{out}}{C_{out}} \cdot 100\% \tag{25}$$

The summary table for all series of experiments is presented below (Table 5). The results for each series will be discussed separately.

Table 5. Consolidated table of experiments.

| Series of experiments | Specific residence time, s $cm^{-2}$ | Relative humidity, % | Inlet concentration, ppm | Ozone, 46-70 ppm |
|---|---|---|---|---|
| 1 | 0.065 and 0.13 | 5 | 20 | with and without |
| 2 | 0.065 | 5 and 40 | 20 | with and without |
| 3 | 0.065 | 5 | 20, 40 and 60 | with and without |

The reference experiments were conducted before the study of influence of operating parameters on the PCO of acetone. They allowed to follow the role of ozone in experimental series. The experimental test with ozone in the dark conditions without catalyst showed no degradation of ozone. Also, no degradation of ozone was monitored in test with ozone under UVA without catalyst in either dry or humid conditions. The full degradation of ozone was reached in reference experiments with catalyst under UVA and dry air. No degradation of acetone was found in presence of ozone in absence of UVA and catalyst. In reference experiment of acetone dark adsorption, no significant adsorption was observed in the continuous reactor under study.

During all the experimental runs, the observed acetone degradation reaction gas-phase products were only carbon dioxide and water; other gas-phase intermediate products were not detected.

## 3.1 Influence of specific residence time

In the first series of experiments, the influence of SRT on the degradation of acetone vapour in presence and in absence of ozone was analysed. The gas flow regime in the section of a reactor influences the distribution of polluted gas upon a catalyst surface. The way, in which fluids move through section can be characterised by Reynolds number (Re). Gas flow in the reactor section can be seen as the flow in the rectangular pipe and gas as the Newtonian fluid. As the acetone

concentration is not high (≤ 0.006 vol.%) and does not influence significantly the air viscosity and density, then in the calculations of Re the properties of pure air can be used.

To characterise the gas flow regime inside the section of the reactor, the Equation 26 can be used:

$$Re = \frac{\rho \cdot V \cdot L}{\mu} \tag{26}$$

Where: ρ - density of the fluid, kg $m^{-3}$

V - characteristic velocity of the flow, m $s^{-1}$

L - characteristic length scale of flow, m

μ - dynamic viscosity of fluid, Pa s

The values of air viscosity and density [35] were linearly interpolated for the reactor temperature of 44 °C using the data given for 40 and 45 °C. The Equation 27 is the equation for linear interpolation.

$$y_2 = \frac{(x_2 - x_1)(y_3 - y_1)}{(x_3 - x_1)} + y_1 \tag{27}$$

The air viscosity at 44 °C (Equation 28):

$$\mu = \frac{(44-40)\left((1.9379-1.9148)\cdot 10^{-5}\right)}{(45-40)} + 1.9148 \cdot 10^{-5} = 1.93328 \cdot 10^{-5}\ [Pa\ s\ ] \tag{28}$$

The air density at 44 °C (Equation 29):

$$\rho = \frac{(44-40)(1.1098-1.1275)}{(45-40)} + 1.1275 = 1.11334\ [kg\ m^{-3}] \tag{29}$$

The section of the reactor can be taken as a rectangle with sizes 4 x 30 x 1.08 cm (width, length and height, respectively). Then cross-sectional area of reactors (Equation 30):

$$A = 4 \cdot 1.08 = 4.32\ [cm^2] \tag{30}$$

To calculate the velocity of gas through an object (pipe, reactor) following equation can be used (Equation 31):

$$Velocity = \frac{Gas\ flow\ rate}{Cross - sectional\ area} \tag{31}$$

Gas velocity at gas flow rate of 0.5 l $min^{-1}$ or 500 $cm^3$ $min^{-1}$ or in terms of residence time 15.6 s per section (Equation 31a):

$$V_{15.6\,\mathrm{s}} = \frac{500}{4.32} = 116\ cm\ \ min^{-1} = 0.019\ [m\ s^{-1}] \qquad (31a)$$

Gas velocity at gas flow rate of 1.0 l $min^{-1}$ or in terms of residence time 7.8 s per section (Equation 31b):

$$V_{7.8\,\mathrm{s}} = \frac{1000}{4.32} = 231\ cm\ \ min^{-1} = 0.0385\ [m\ s^{-1}] \qquad (31b)$$

Characteristic length, L, is the hydraulic diameter, which for the rectangular tube could be calculated as follows (Equation 32, where a and b are the dimensions of the reactor section, mentioned above):

$$L = \frac{4 \cdot a \cdot b}{2(a+b)} = \frac{4 \cdot 0.04 \cdot 0.0108}{2(0.04 + 0.0108)} = 0.017\ [m] \qquad (32)$$

With these values, the Re can be found for both flow rates (Equations 25a and 25b).

$$Re_{0.5\,\mathrm{l\,min^{-1}}} = \frac{1.11334 \cdot 0.019 \cdot 0.017}{1.93328 \cdot 10^{-5}} = 19 \qquad (26a)$$

$$Re_{1.0\,\mathrm{l\,min^{-1}}} = \frac{1.11334 \cdot 0.0385 \cdot 0.017}{1.93328 \cdot 10^{-5}} = 38 \qquad (26b)$$

Table 6. Reynolds Numbers for different types of flow.

| **Flow type** | **Reynolds Number range** |
|---|---|
| Laminar regime | up to Re = 2300 |
| Transition regime | 2300 < Re < 4000 |
| Turbulent regime | Re > 4000 |

According to Reynolds Numbers for different flow types (Table 6), the gas flow regime in the reactor is laminar. It means that viscous forces are higher than inertial forces and that enables gas to flow in parallel layers without mixing. This way the air with acetone molecules moves orderly in the flow in straight lines parallel to catalyst surface spreading pollutant evenly. Even spreading of pollutant on a catalyst surface provides equal load on the active centres, which

allows catalyst to function to full capacity. The full mixing of the air moving through the reactor is supposed to happen between the sections due to the changes in air velocity (tubing and specific space near the outlets of the sections).

If the gas flows through section too fast, then the residence time will be too short and there will be not enough time for all molecules of acetone to take part in photocatalytic reactions on the or in the vicinity of the surface of the catalyst. Thus, the longer residence times are beneficial for the chemical reactions, but the treatment of large volumes of polluted gas becomes technically and economically problematic. The addition of ozone as supplementary oxidant to the photocatalytic system could sometimes accelerate the degradation of target pollutants.

In Figure 10, the dependence of acetone conversion on residence time is presented. At the same SRT (0.065 or 0.13 s $cm^{-2}$) the presence of ozone indeed accelerate the acetone degradation process, as higher conversions are achieved faster. For example, without ozone, the acetone conversion of 70% is achieved after 7.8 s (SRT of 0.065 s $cm^{-2}$), but in presence of ozone this is at least 10% higher. Approximately 16 s (two sections of reactor) are needed to degrade acetone in presence of ozone, while ca. 32 s (four sections of reactor) are required to degrade the same amount of acetone in absence of ozone at shorter SRT of 0.065 s $cm^{-2}$. As ozone is totally degraded (zero content in the outlet of the reactor), the acceleration of the process occurs due to the enhanced number of oxygen and hydroxyl radicals formed within the photocatalytic reactors.

The construction of reactor allows to compare the conversions of pollutant at the same residence time but different air flow regimes (different SRT). For instance, one section of reactor at SRT of 0.13 s $cm^{-2}$ gives as a result 15.6 s of residence time, while two sections of reactor at SRT of 0.065 s $cm^{-2}$ result in same 15.6 s for the acetone molecules. Data received at the same residence time and different air flow regimes is seen in Figure 10 at 15.6 and 31.2 s: different air flows and same residence time result in the same acetone conversions despite different areas of photocatalytic surfaces.

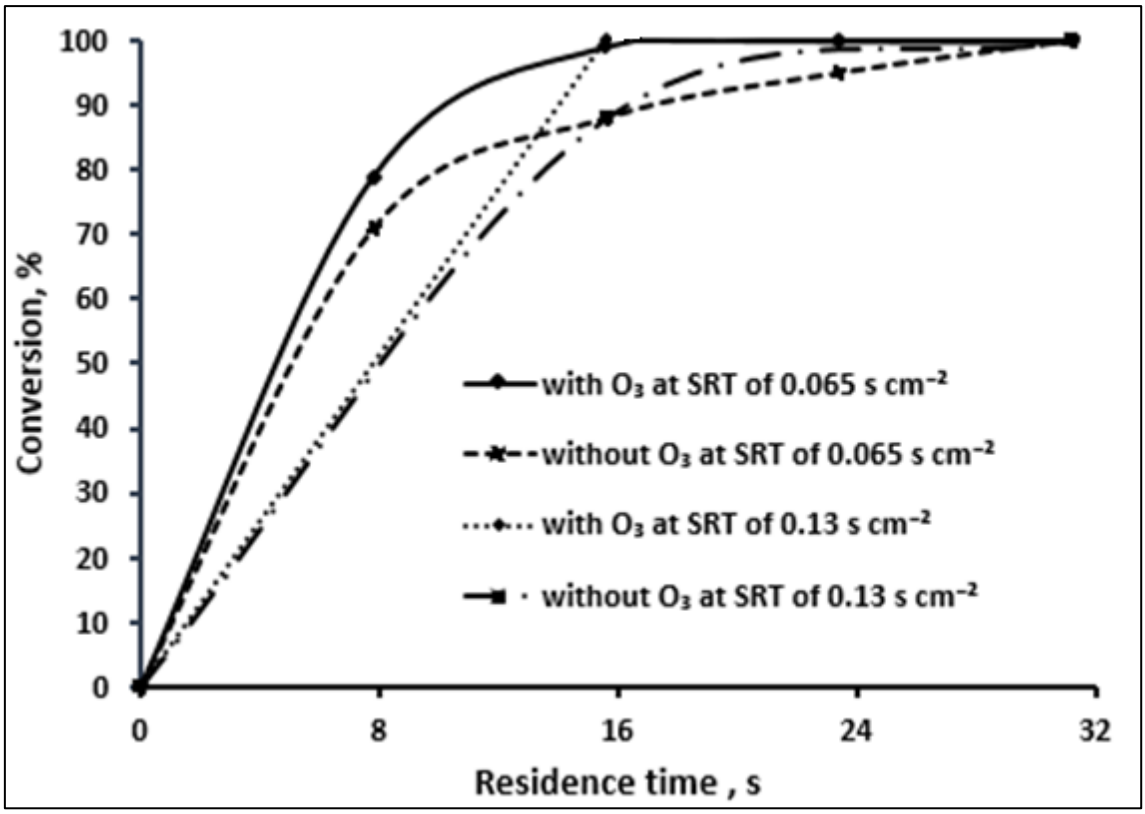


Figure 10. Influence of residence time on process performance (acetone initial concentration 20 ppm, RH 5%).

Altogether, flow regime is supposed to have an impact on the performance of photocatalytic reactions: this parameter influences the overall mass transfer, the distribution of acetone molecules upon catalyst surface and, thus, the occupation of catalyst active centres. However, the two-time decrease in SRT (from 0.13 to 0.065 s $cm^{-2}$) does not influence the photocatalytic process performance in presence or in absence of ozone. As was ascertained above both flow regimes are laminar.

## 3.2 Influence of air humidity

In the second experimental series, the influence of air humidity on acetone conversion values was studied. During these experimental runs, the degradation of 20 ppm of acetone was carried out at RH of 5 and 40%; the experiments were made at SRT 0.065 and 0.13 s $cm^{-2}$ without and with addition of $O_3$.

Increase in air humidity intensifies competition for adsorption between acetone and water molecules on the catalyst surface. On one hand, just as acetone, the water molecules also adsorb

on a catalyst surface and form hydroxyl radicals (•OH) that react with acetone. Additional •OH improve acetone degradation and boost mineralization towards $CO_2$ and $H_2O$. On the other hand, presence of larger amount of water vapour has a significant negative effect on the photocatalytic process performance, as adsorption of water molecules may block some active sites, thus resulting in lesser amount of adsorbed acetone and lower rates of its oxidation.

The results of first set of experiments in presence and in absence of $O_3$ at SRT of 0.065 s $cm^{-2}$ are presented in Figures 11 and 12. It can be seen, that increase in air humidity resulted in a decrease in the acetone conversion values. This is especially noticeable on photocatalytic surface area of 120 and 240 $cm^2$. According to the obtained data, 120 $cm^2$ of photocatalytic surface and time of 7.8 s are not enough for full degradation of acetone and higher humidity decrease it for approximately 20%. Then, increase in photocatalytic surface area and residence time lessened the difference in pollutant's conversion values. The full conversion at both humidity levels was reached on surface area of 480 $cm^2$. Raise of conversion values with expansion of surface area can be explained by the increase in the amount of catalyst active sites. Vast number of sites allows to lessen competition between acetone and water molecules levelling the negative effect of water vapour.

The addition of $O_3$ along with the increase in humidity has no effect on the acetone conversion values. At higher humidity (40%, Figures 11 and 12) the acetone conversion values in absence and presence of ozone are almost the same, having only negligible difference at the lowest residence time (one section, 120 $cm^2$, conversion 53 and 58%). The absence of ozone promotive effect at higher air humidity could be explained by the reaction of radicals formed during the ozone degradation mostly with water molecules and not with acetone as well as recombination of radicals can be presumed.

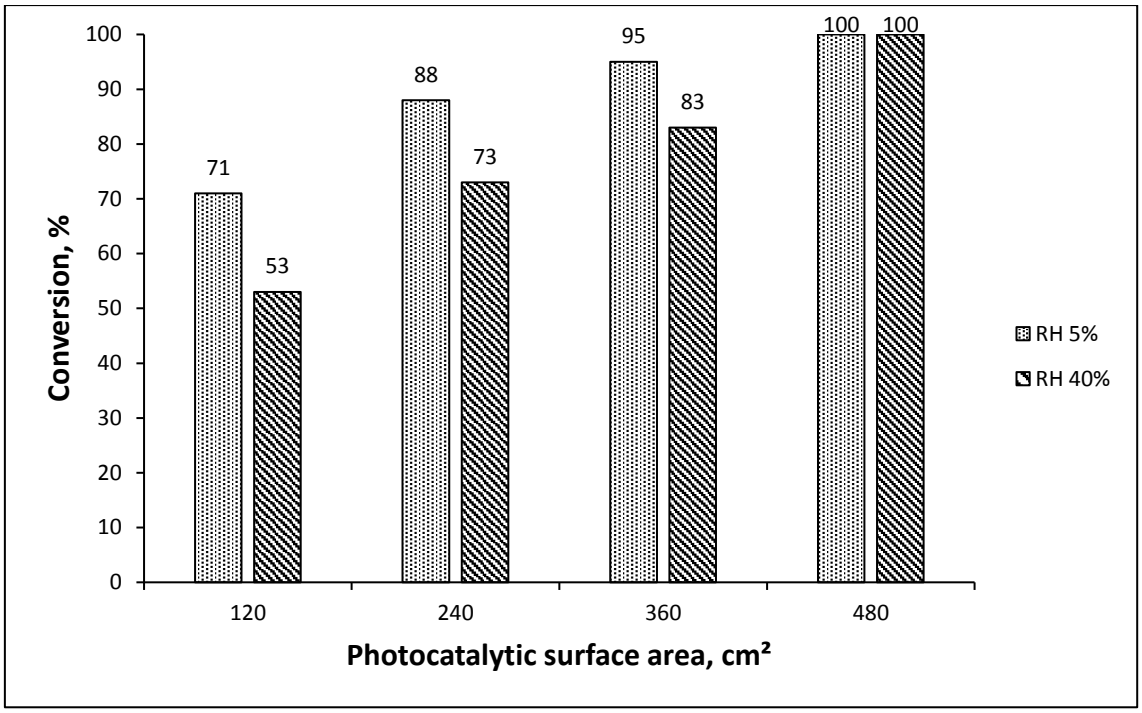


Figure 11. Influence of relative air humidity on process performance at specific residence time 0.065 s $cm^{-2}$, without $O_3$ (acetone initial concentration 20 ppm).

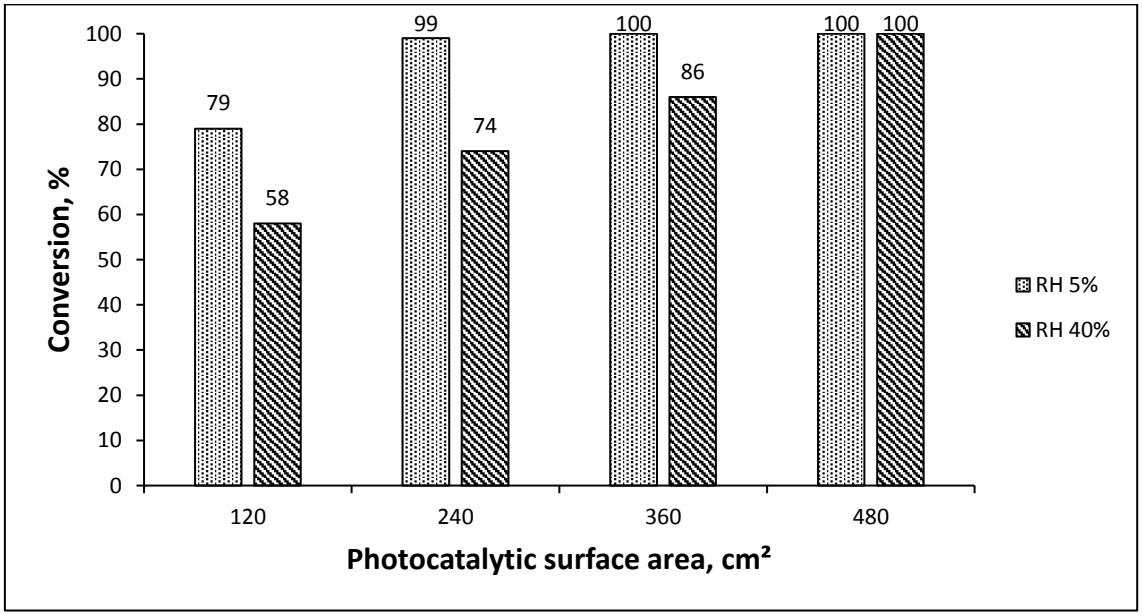


Figure 12. Influence of humidity on process performance at specific residence time 0.065 s $cm^{-2}$, with $O_3$ (acetone initial concentration 20 ppm).

The results of the experimental runs with higher air humidity at SRT of 0.13 s $cm^{-2}$ with and without $O_3$ are presented in Figures 13 and 14. If compared with the results in Figure 11 and 12, it can be seen, that prolonged SRT raised overall conversion values considerably for both humidity conditions. However, the overall effect of the higher humidity is still negative despite the twice as longer residence time in the reactor section. As observed previously, the raise of

humidity lessened the conversion value. In addition, the 100% acetone conversion was obtained at photocatalytic surface area of 360 $cm^2$ (at residence time of ca. 47 s) under more humid conditions as well. Thus, at prolonged residence time the smaller photocatalytic surface could be enough for the total degradation of pollutant at RH 40%. The increase in photocatalytic surface area, again, noticeably reduced the difference in conversion rates at different conditions of humidity.

The presence of ozone at longer SRT favours slightly the acetone oxidation under less and more humid conditions: conversion values are increased by 9 and 10% in the first section of reactor, respectively (Figures 13 and 14). However, it could be concluded that ozone effect at higher humidity is either negligible or absent. The competition between acetone and water molecules takes place.

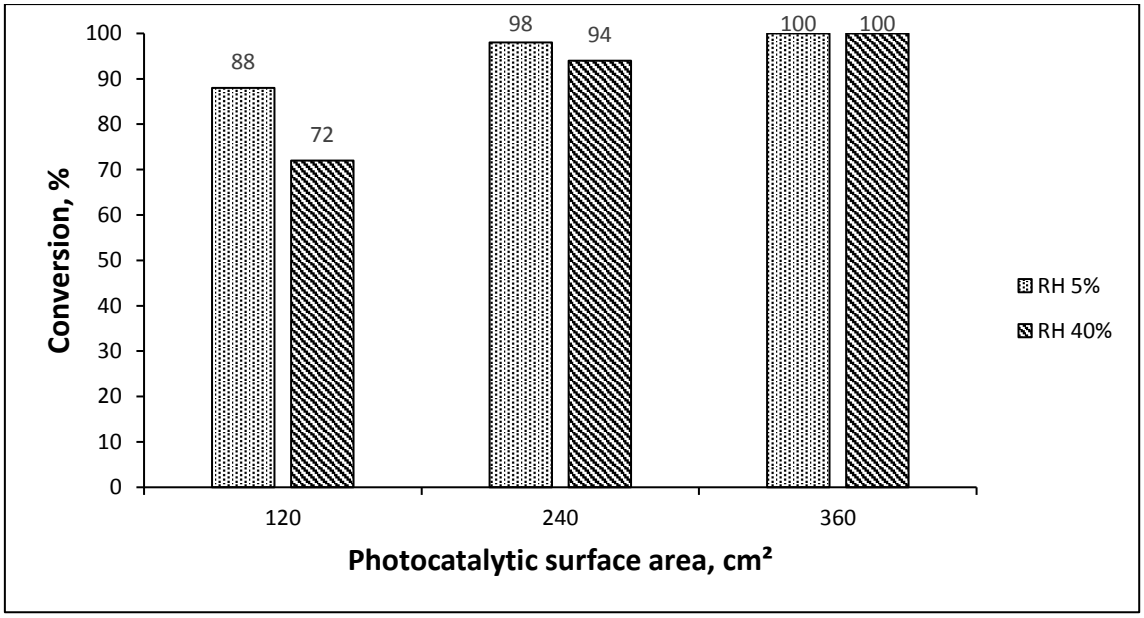


Figure 13. Influence of humidity on process performance at specific residence time 0.13 s $cm^{-2}$, without $O_3$ (acetone initial concentration 20 ppm).

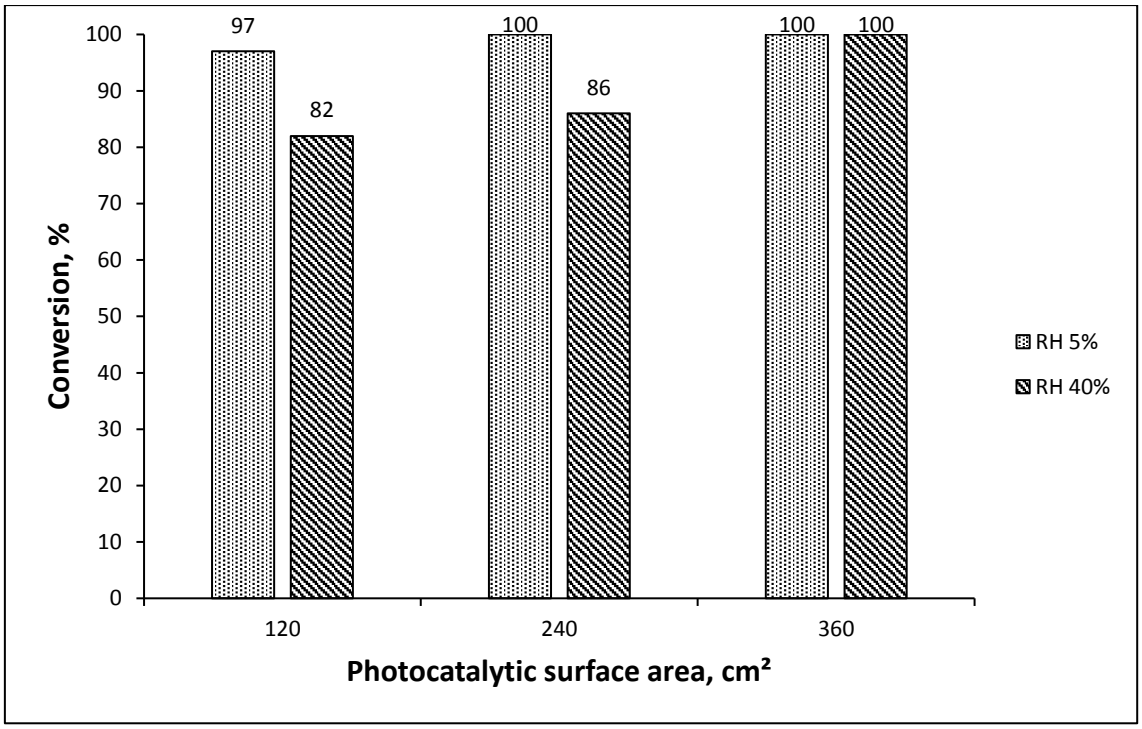


Figure 14. Influence of humidity on process performance at specific residence time 0.13 s $cm^{-2}$, with $O_3$ (acetone initial concentration 20 ppm).

## 3.3 Influence of inlet concentration of acetone

The PCO process depends among the other parameters discussed above on the amount of catalyst and inlet concentration of pollutants. The kinetics of heterogeneous photocatalytic processes is very complex, as this includes generation of reactive species (radicals) by the catalyst under radiation, adsorption of initial pollutants and their degradation, formation of oxidation intermediate products and their adsorption-desorption equilibria, oxidation of intermediate products. Dual role of water vapour was discussed in previous section. The amount of pollutants usually influences the kinetics of reaction, which influences overall performance of the process. In heterogeneous photocatalysis, usually the increase in pollutant concentration decreases the conversions of initial pollutant. High concentration of pollutant leads to the saturation of catalyst active cites by the organic molecules of initial or intermediate compounds and that reduces catalyst's activity, in some cases deactivates it. At higher concentrations of pollutants, the process becomes to be limited by the generation of charge carriers and reactive species by the catalyst, and in that case, the further increase in inlet pollutant concentration does not result in increased amount of degraded compounds.

In the experimental series presented in this section, the effect of initial concentration on the conversion and amount of degraded acetone was studied. The initial concentrations of acetone were 20, 40 and 60 ppm. The results obtained in the absence of ozone are reported in Figure 15. The increase in acetone inlet concentration 3 times from 20 to 60 ppm resulted in no changes in acetone conversions at the lowest residence time of 7.8 s (one section, 120 $cm^2$). Moreover, with the increase in residence time and photocatalytic surface area no influence of the increase in acetone inlet concentration on the acetone conversions was still observed. At 360 $cm^2$ (23.4 s) over 95% conversion of acetone at concentrations of up to 60 ppm was achieved.

If considering not the conversions, but the amount of acetone, than in 7.8 s (one section) – ca. 14 ppm (0.71*20), 29 ppm (0.72*40) and 42 ppm (0.7*60) of acetone are degraded. Thus, the increase in the initial concentration of acetone leads to the almost proportional increase in the amount of the degraded pollutant at lower residence time (ca. 8 s) and the degraded amount is proportional to the initial concentrations at longer residence time (> 20 s): 20, 40 and 60 ppm of acetone are degraded at respective inlet concentrations.

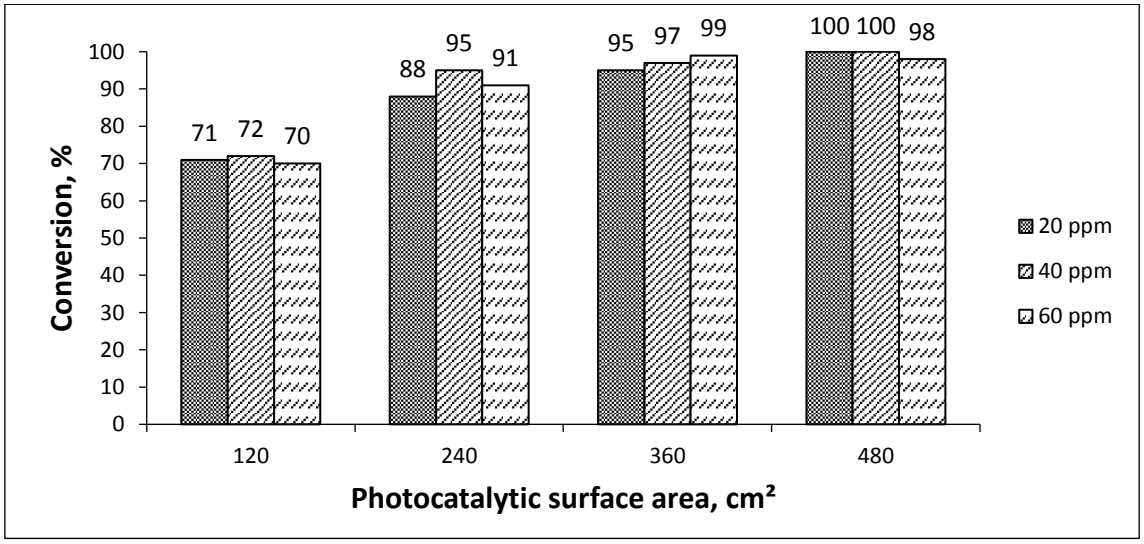


Figure 15. Influence of acetone concentration on process performance, without $O_3$ (specific residence time 0.065 s $cm^{-2}$, RH 5%).

The results of photocatalytic degradation of 20, 40 and 60 ppm of acetone in presence of $O_3$ are presented in Figure 16. As was observed previously, in case of 20 ppm the addition of ozone promoted the acetone oxidation at SRT of 0.065 s $cm^{-1}$. However, addition of $O_3$ to the photocatalytic system, where acetone inlet concentration were 40 and 60 ppm, did not promoted the overall oxidation. Moreover, in presence of ozone the acetone oxidation process was slightly deteriorated at the shortest residence time of 7.8 s. It can be attributed to the fact, that ozone degradation is initiated by the photocatalyst active sites and at higher acetone

concentrations ozone molecules are in more tight competition with acetone for those cites. The positive effect of additional generation of reactive oxygen species by low ozone content in air (about 100 μg $l^{-1}$) does not affect the overall acetone degradation as this effect is supposed to be opposed by the negative influence of acetone desorption or hindered adsorption.

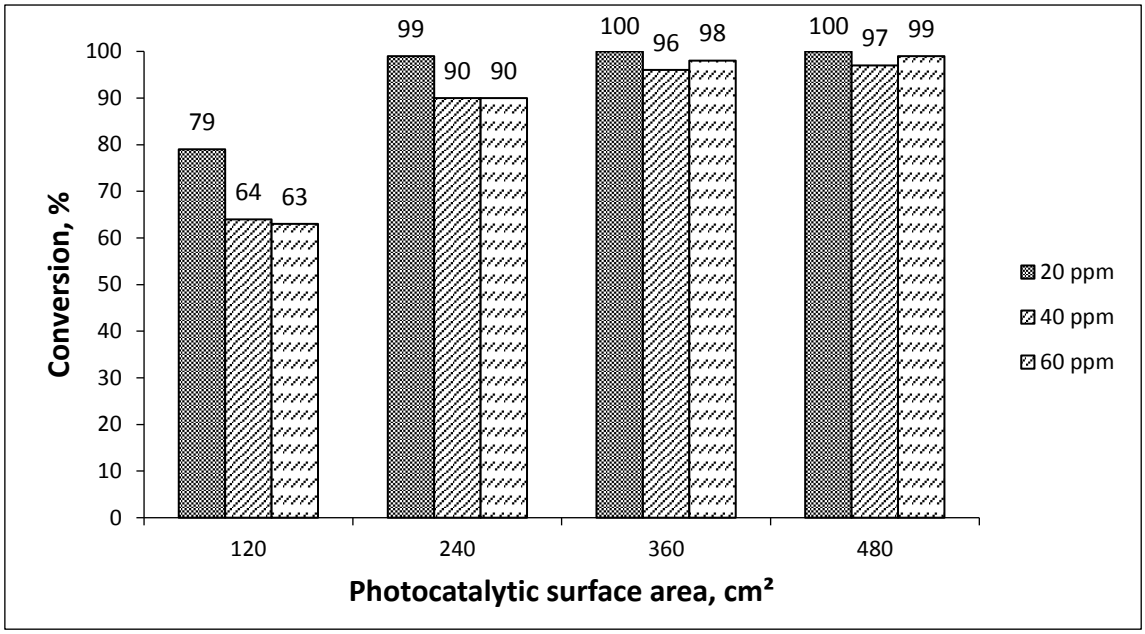


Figure 16. Influence of acetone concentration on process performance, with $O_3$ (specific residence time 0.065 s $cm^{-2}$, RH 5%).

As a result of these experimental runs, it is observed, that with the increase in initial concentration of acetone the amount of degraded substance is increased proportionally to the concentration rise in the range of studied concentrations (20-60 ppm). Thus, it can be concluded that the active sites of the catalyst and overall generation of radicals, amount of photocatalyst, intensity of UVA light allow to mineralize at least up to 60 ppm of acetone in less than 35 s.

# 4. CONCLUSIONS

The influence of ozone on the photocatalytic oxidation of acetone on P25 $TiO_2$ coatings in multi-sectional continuous reactor was studied. Photocatalytic oxidation of acetone under different operating conditions was carried out: specific residence time, humidity and initial acetone concentrations were varied. Application of P25 $TiO_2$ photocatalytic coating allowed achieving 100% conversion of acetone with no gas-phase oxidation products other than $CO_2$ and $H_2O$.

The studied air flow regimes in reactor were characterised as laminar. The obtained data indicated that decrease in specific residence time from 0.13 to 0.065 s $cm^{-2}$ did not influenced the photocatalytic process performance in presence or in absence of ozone at the same residence time with the increase in photocatalytic surface area. Longer residence time at the same photocatalytic surface increased the photocatalytic conversions of acetone. Addition of ozone at lower acetone concentration (20 ppm) favoured the photocatalytic process performance at different specific residence times.

The increase in air humidity (from 5 to 40% of relative humidity) decreased acetone conversion values at lower residence times. The conversion values lessened with the increase in air humidity as the competition between acetone and water molecules was augmented. However, the longer residence times allowed obtaining complete acetone degradation at higher air humidity values. Ozone effect at higher humidity is either negligible or absent.

Raise of acetone initial concentration (from 20 to 60 ppm) showed the proportional increase in the amount of degraded substance, where the conversions of acetone remained nearly unchanged. The enhancement effect of ozone was not observed at higher acetone inlet concentrations (40-60 ppm).

# Resümee

Tehnoloogia arengu ja üldise tootmise suurenemise tingimustes on õhu puhastamise vajadus muutunud üheks keeruliseks probleemiks. Lenduvate orgaaniliste ühendite heitkoguste vähendamise meetodid on erinevad: kondensatsioon, absorptsioon, adsorptsioon, termiline oksüdatsioon. Fotokatalüütiline oksüdatsioon on tehnoloogia, mida saab kasutada õhu puhastamiseks. See tehnoloogia on võimeline hävitama orgaanilisi osakesi suurusega umbes 0,001 mikronit, mikroobe ning lagundama lenduvaid orgaanilisi ühendeid.

Käesoleva töö eesmärk oli atsetooniauru lagundamine fotokatalüütilise oksüdeerimise abil koos titaanoksiidi katalüsaatoriga ultraviolettkiirguse toimel pidevas mitmesektsioonilises reaktoris. Uuriti fotokatalüütilise oksüdeerimise ja osooni kombinatsioone erinevates töötingimustes, et hinnata osooni võimendavat toimet.

Saadud tulemuste põhjal võib järeldada, et eriviibeaja vähenemine ei mõjuta fotokatalüütilise protsessi toimivust osooni juuresolekul või selle puudumisel sama viibeaja jooksul fotokatalüütilise pindala suurenemisel. Õhuniiskuse suurenemine vähendab atsetooni konversiooni madalamatel viibeaegadel. Atsetooni algkontsentratsiooni tõusuga suureneb proportsionaalselt lagunenud aine kogus.

# References


1. NSW Government, Environmental Health (2013). *Outdoor air pollution* https://www.health.nsw.gov.au/environment/air/Pages/outdoor-air-pollution.aspx (10.11.2018)

2. ChemSafety PRO (2018). *Volatile Organic Compounds (VOC) and Consumer Products Regulations* https://www.chemsafetypro.com/Topics/VOC/What_Are_Volatile_Organic_Compounds_(VOC)_and_Overview_of_Global_VOC_Regulations.html (4.03.2019)

3. Air Pollution Information System (2016). *Volatile Organic Compounds.* http://www.apis.ac.uk/overview/pollutants/overview_VOCs.htm (23.02.2019)

4. Guenther A., Hewitt C.N., Erickson D., Fall R., Geron C., Graedel T., Harley P., Klinger L., Lerdau M., McKay W.A., Pierce T., Scholes B., Steinbrecher R., Tallamraju R., Taylor J. and Zimmerman P. (1995). A global model of natural volatile organic compound emissions. *Journal of Geophysical Research,* vol. 100, issue 5, p. 8873-8892. doi: 100. 8873-8892. 10.1029/94JD02950

5. Zhang R., Mitloehner F.,El-Mashad H., Malkina I., Rumsey T., Arteaga V., Zhu B., Zhao Y. (2010). Process-Based Farm Emission Model for Estimating Volatile Organic Compound Emissions from California Dairies. *ResearchGate.* https://www.researchgate.net/publication/287723762_Process-Based_Farm_Emission_Model_for_Estimating_Volatile_Organic_Compound_Emissions_from_California_Dairies (04.03.2019)

6. Lund H. (ed) (1971). *Industrial pollution control handbook*, p.14-17. (19.2019)

7. Guigard S., Kindzierski W., Purtill C., Schulz J., Treissman D., Vidmar J. (2004). *Assessment Report on Acetone for Developing Ambient Air Quality Objectives*. Pub. No: T/748 (19.02.2019)

8. Patterson R., Bornstein M., Garshik E. (1976*).* Assessment of Acetone as a Potential Air Pollution Problem. *EPA,* vol. 5, CCA-TR-75-32-G(5). (21.11.2018)

9. Gondalez M. (2019). The production rate of acetone per year of plant. *ICIS Plants & Projects.*

https://www.academia.edu/3807341/The_production_rate_of_acetone_per_year_of_plant (4.03.2019)

10. Kalfas J. (2016). *Emissions Calculations.* p.15-17 (4.03.2019)

11. Lagzi I., Mészáros R., Gelybó G., Leelőssy A. (2013). Atmospheric Chemistry. Gaussian Dispersion model. *Elte TTK, TÁMOP-4.1.2.A/1-11/1-2011-0073.* http://elte.prompt.hu/sites/default/files/tananyagok/AtmosphericChemistry/ch10s03.html (4.03.2019)

12. College of Engineering OSU Extended Campus (2004). *Gaussian Plume model*. https://courses.ecampus.oregonstate.edu/ne581/eleven/plume.htm (4.03.2019)

13. Williams & Marshall Strategy (2019). *The Global Acetone Market*. https://www.researchandmarkets.com/research/vff8tr/the_global?w=4 (22.02.2019)

14. Miller F., Silva C., Brandão T. (2013). A Review on Ozone-Based Treatments for Fruit and Vegetables Preservation. *Food Engineering Reviews,* vol. 5, issue 2, p.77-106. (21.02.2019)

15. Air Pollution Information System (2016). *Ozone.* http://www.apis.ac.uk/overview/pollutants/overview_O3.htm (21.02.2019)

16. Allen J. (2002). *Chemistry in the Sunlight*. https://earthobservatory.nasa.gov/features/ChemistrySunlight/chemistry_sunlight3.php (10.03.2019)

17. Verma N. (2014). An investigation of Ozone formation through its precursors (CO; NOx; VOC) and its loss at a sub-urban site of Agra. *SemanticScholar*. (13.03.2019)

18. Article shared by Shantanu Baner. Abatement Methods of VOCs | Air Pollution. *Your Article Library*. http://www.yourarticlelibrary.com/air-pollution/abatement-methods-of-vocs-air-pollution/78292 (23.11.2018)

19. Gupta V., Verma N. (2002). Removal of Volatile Organic Compounds by Cryogenic Condensation Followed by Adsorption. *Chemical Engineering Science*, vol. 57, p. 2679-2696. doi: 10.1016/S0009-2509(02)00158-6

20. EMIS (2015). *Recuperative telmal oxidation*. https://emis.vito.be/en/techniekfiche/recuperative-thermal-oxidation (21.02.2019)

21. EMIS (2015). *Regenerative thermal oxidation*. https://emis.vito.be/en/techniekfiche/regenerative-thermal-oxidation (22.02.2019)

22. Evans L., Vatavuk W., Stone D., Lynch S., Pandullo R., Koucky W. (2000). VOC Destruction Controls, Flares. *VOC controls*, Chapter 1. p.3., EPA/452/B-02-001 (20.02.2019)

23. Huang Y., Sai Hang Ho S., Lu Y., Niu R., Xu L., Cao J., Lee S. (2016). Removal of Indoor Volatile Organic Compounds via Photocatalytic Oxidation: A Short Review and Prospect. *Molecules*, 21, 56. doi:10.3390/molecules21010056

24. Thiruvenkatachari R., Vigneswaran S., Shik Moon I. (2008). A review on UV/TiO2 photocatalytic oxidation process. *Korean Journal of Chemical Engineering*, vol. 25, issue 1, p. 64-72. doi: 10.1007/s11814-008-0011-8

25. Zhang M., Chenb T., Wang Y. (2017). Insights into TiO2 polymorphs: highly selective synthesis, phase transition, and their polymorphdependent properties. *Royal Society of Chemistry Advances*, vol.7, 52755. doi: 10.1039/c7ra11515f

26. SIDS initial assessment profile (2013). *Titanium dioxide* . https://hpvchemicals.oecd.org/UI/handler.axd?id=1f6be49d-48b6-4909-8e0d-a6f5e48503d3 (28.03.2019)

27. Shena S., Kronawitterb C., Kiriakidis G., (2017). An overview of photocatalytic materials. *Journal of Materiomics*, vol. 3, issue 1, p. 1-2. (28.03.2019)

28. Mamaghani A., Haghighat F., Lee C. (2017). Photocatalytic oxidation technology for indoor environment air purification: The state-of-the-art*. Applied Catalysis B:* Environmenta, vol. 203, p. 247-269. (25.03.2019)

29. Kumar A., Pandey G. (2017). A Review on the Factors Affecting the Photocatalytic Degradation of Hazardous Materials*. Material Science & Engineering International Journal*, vol. 1, issue 3, p.1-2. (27.03.2019)

30. Choi W., Yun Ko J., Park H., Shik Chung J. (2000). Investigation on TiO2-coated optical fibers for gas-phase photocatalytic oxidation of acetone. *Applied Catalysis B: Environmental*, vol. 31, p. 209–220. (29.03.2019)

31. Yu K., Lee G. (2007). Decomposition of gas-phase toluene by the combination of ozone and photocatalytic oxidation process (TiO2/UV, TiO2/UV/O3, and UV/O3). *Applied Catalysis B: Environmental*, vol. 75, issues 1-2, p. 29-38. doi: 10.1016/j.apcatb.2007.03.006

32. Yu K., Lee G., Huang G. (2010). The effect of ozone on the removal effectiveness of photocatalysis on indoor gaseous biogenic volatile organic compound. *Journal of the Air & Waste Management Association*, vol. 60, issue 7, p. 820-829. doi: 10.3155/1047-3289.60.7.820

*33.* Huang H. (2010). Removal of Air Pollutants by Photocatalysis with Ozone in a Continuous-Flow Reactor. *Environmental Engineering Science*, vol. 27, issue 8. doi: 10.1089/ees.2009.0392

34. Ohtani B., Prieto-Mahaney O., Li D., Abe R. (2010). What is Degussa (Evonik) P25? Crystalline composition analysis, reconstruction from isolate pure particles and photocatalytic activity test. *Journal of Photochemistry and Photobiology A Chemistry*. vol. 216, issues 2-3. doi: 10.1016/j.jphotochem.2010.07.024

35. Evans P. (2015). *Properties of Air at atmospheric pressure*. https://theengineeringmindset.com/properties-of-air-at-atmospheric-pressure/ (9.04.2019)